

Beam test of a Time-of-Flight detector prototype.*

J. Va'vra[#], D.W.G.S. Leith, B. Ratcliff

SLAC, Stanford University, CA 94309, U.S.A.^{**}

E. Ramberg, M. Albrow, A. Ronzhin

Fermilab, Batavia, Il 60510, U.S.A.

C. Ertley, T. Natoli

University of Chicago, Chicago, Il 60637, U.S.A.

E. May, K. Byrum

Argonne National Laboratory, Argonne, Il 60439, U.S.A

Elsevier use only: Received date here; revised date here; accepted date here

Abstract – We report on results of a Time-of-Flight, TOF, counter prototype in beam tests at SLAC and Fermilab. Using two identical 64-pixel Photonis Microchannel Plate Photomultipliers, MCP-PMTs, to provide start and stop signals, each having a 1 cm-long quartz Cherenkov radiator, we have achieved a timing resolution of $\sigma_{\text{Single_detector}} \sim 14$ ps.

To be published in Nucl. Instr.& Methods

• Manuscript received on March 25, 2009.

[#] Corresponding author. tel.: 650-926-2658; fax: 650-926-4178; e-mail: jjv@slac.stanford.edu.

^{**} Work supported by the Department of Energy, contract DEAC02-76SF00515

1. Introduction

This paper reports on the performance of a novel time-of-flight, TOF, technique using a quartz radiator, and a fast photodetector coupled to 1 GHz bandwidth (BW) electronics.

We present¹ new timing measurements with the Photonis 85011 MCP-PMT (micro-channel plate PMT) with 10 μm holes. Each PMT had an 8x8 array of 6mm x 6mm anode pads. We used two identical detectors (Fig. 1a), both equipped with the same electronics. The setup was tested in the SLAC and Fermilab test beams. The same detectors were also used in laser diode tests [1].

We considered two possible choices of the Cherenkov radiator: (a) segment the radiator into cubes, each concentrating the light on small number of pads (four pads connected together in these tests). In this case the detector has a larger signal and can operate at lower gain, or (b) the non-segmented radiator is part of the MCP-PMT window (so called “stepped face” Photonis MCP-PMT), with all 64 pads instrumented. In this case the Cherenkov light from the single particle populates up to 16 pads and the typical charge per pad is only a few photoelectrons, therefore the detector needs to operate at higher gain. In this paper we describe tests simulating the first option only, although a test of the second option is under way.

We operated both MCP-PMTs at a low gain ($\sim 2 \times 10^4$), where the detector is not sensitive to single photoelectrons, however it has a linear response in the range of number of photoelectrons ($N_{pe} \sim 35 \pm 5$). This is a departure from the previous method [2], where we operated in the single photoelectron mode. We believe that a low gain operation will help the aging and rate issues in high rate applications².

This TOF detector is being considered as a possible option for a Super-B particle identification, PID, detector [3] in the forward regions. Generally, a

¹ Presented also at IEEE, Dresden, October 25, 2008.

http://www.slac.stanford.edu/~jjv/activity/Vavra_Dresden_talk.pdf

² Initial laboratory tests are consistent with this hypothesis. Such a detector does not see a single photoelectron background, it is sensitive only to charged particles. These tests are in progress.

TOF-based PID is competitive with a RICH PID up to a momentum of ~ 4 GeV/c, if one has at least 2 m of TOF path: for example, (a) with $\sigma_{\text{TOF}} \sim 5\text{-}10$ ps one can compete with an Aerogel RICH ($n \sim 1.03$), or, (b) with $\sigma_{\text{TOF}} \sim 15\text{-}20$ ps one can compete with a DIRC-like RICH ($n \sim 1.47$ [3]). However, the TOF technique cannot compete with a gaseous RICH at higher momenta.

For a Super-B PID application, the detector must work at 16 kG, which means that the MCP hole diameter must be 10 μm or less [4].

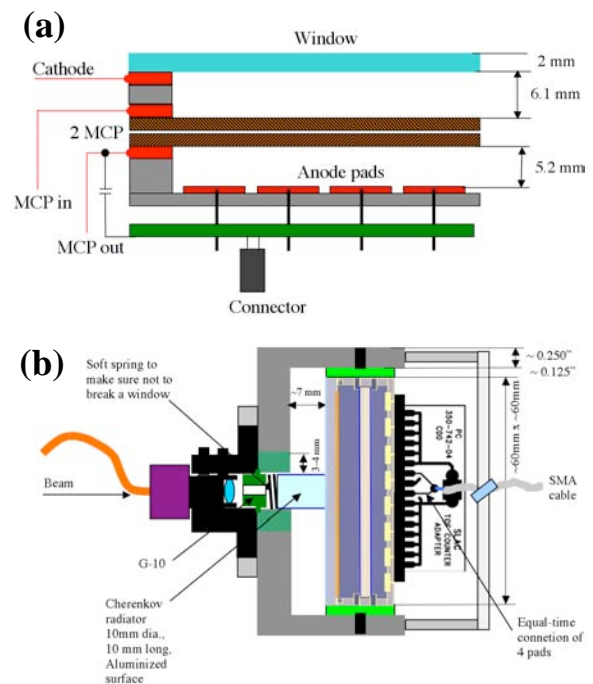


Fig. 1. (a) Cross-section of the MCP-PMT 85011 used in our tests. (b) Two identical detector setups were built to allow a relative start-stop measurement using either a laser or a beam. Each detector has a fiber connector for the laser diode calibration (in the beam we remove the fiber to reduce the mass). The picture also shows a 1cm long quartz radiator, coupled to the MCP window with an optical grease.

2. Experimental setup.

Fig.1b shows the MCP-PMT enclosure with a fused silica radiator (10 mm dia., 10 mm long) and fiber optics. The MCP-PMT has 64 pads; four pads under the radiator were shorted together and

connected to an amplifier. The other pads were shorted to ground. Two identical MCP-PMT detectors were prepared, both having 10 μm dia. holes³. Fig.2a shows the wavelength bandwidth of the TOF1 detector. Peak quantum efficiencies at 420 nm for both TOF detectors are shown in Fig.2b, together with other MCP detector examples. Based on integration in Fig.2a, the expected numbers (N_{pe}) are ~ 30 for the TOF1 and 42 for the TOF2 counters, assuming a 10 mm long quartz radiator and the Photonis Bialkali photocathode data for the two tubes.⁴ We will assume an average of the two, $N_{\text{pe}} = 35 \pm 5$.

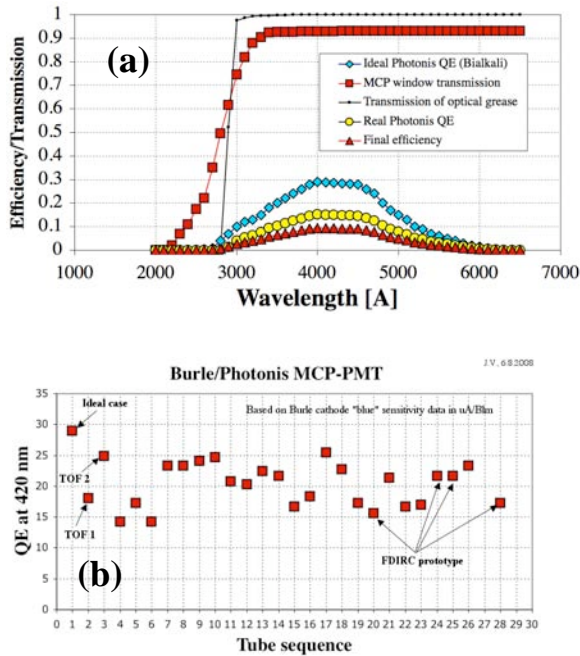


Fig. 2 (a) An estimate of the wavelength bandwidth of the presented TOF1 detector. (b) Typical peak QE at 420 nm scaled from the Photonis “ideal” QE using the “blue” sensitivity in $\mu\text{A}/\text{Blm}$ for each tube.

³ Two Burle/Photonis MCP-PMTs, S/N: 11180401 & 7300714.

⁴ N_{pe} is calculated using various known efficiencies and transmissions, including the real QE based on the luminous sensitivity for both detectors provided by the Photonis.

The electronics⁵ used in the SLAC tests and its pulser⁶ calibration is shown on Fig.3a. Fig.3b shows the resulting time calibration of the Ortec TAC/ADC system. The scope picture of pulses from this pulser is shown in Fig.3c; the pulser produces one start and multiple equally spaced random stops. The result of this calibration is 3.19 ps/count. The Fermilab electronics was the same as in the SLAC laboratory and beam tests, with the exception of adding ADCs to monitor the MCP-PMT pulse heights, which allowed additional cuts and time-walk corrections to the constant fraction discriminator, CFD, timing; this proved to be a significant improvement. Fig.3d shows the SLAC laboratory test results together with one point from the Fermilab test, where the output from one detector was used for both Start and Stop branches of the electronics using a high bandwidth splitter⁷. One can see that the Fermilab test beam electronics contribution to a single detector was $\sigma_{\text{Electronics_single_detector}} = \sigma_{\text{Electronics_two_detectors}}/\sqrt{2} \sim 4.6$ ps, i.e. it is somewhat worse than in the SLAC lab test result of $\sigma_{\text{Electronics_single_detector}} \sim 2.5$ ps for the same ADC value of ~ 1800 counts. One can also see that the electronics resolution depends on the ADC count, probably a feature of this particular TAC, i.e., one could reach ~ 2 ps for even smaller ADC values of ~ 500 . The SLAC test operated near ~ 3700 count, while the Fermilab test was operating near ~ 2000 counts. The electronics resolution of 2-3 ps is one of the best results ever achieved, to our knowledge; it means that the electronics noise does not limit our results.

The SLAC End Station A 10 GeV/c electron beam had a spot size of $\sigma \sim 1\text{-}2$ mm [5,6]. The beam pile-up, which is a typical intensity related problem due to SLAC’s short duty cycle, were eliminated with the lead glass. We used the same electronics as in the laboratory tests (Fig.3a). The same laser system was used to calibrate the detectors prior to the particle

⁵ Electronics: Ortec 9327 CFD with 10x internal 1 GHz BW amplification, TAC 588, CFD 9327, 14 bit ADC 114. CFD arming thresholds was -10mV , the CFD walk (zero-crossing) threshold was $+5\text{mV}$.

⁶ 200MHz pulser with one start & multiple equally spaced random stops, made by Impeccable instruments, LLC, Knoxville, Tn., USA, www.ImpeccableInstruments.com.

⁷ Minicircuits, High BW analog splitter ZFRSC-42+.

beam (Fig.3a), and we achieved the same performance in the test beam as in the lab. However, we did not measure the MCP-PMT pulse heights during the beam test, and therefore could not do the off-line ADC-based corrections.

The 120 GeV proton test beam at Fermilab had a larger spot size, but we triggered on a small scintillator 2 mm x 2 mm size viewed by two PMTs. The electronics was the same as in the SLAC tests, however it included the ADC measurement on the MCP-PMT pulses – see Fig.4. In addition, the test had a 2 mm scintillator defining a small “in-time” beam spot. The electronics setting was the same as in the SLAC beam test.

Both beam tests used the nominal Photonis-recommended resistor chain⁸ [1]. Fig.5c shows the gain dependencies of the two detectors⁹. We run detectors at the low gain of $\sim 2 \times 10^4$.

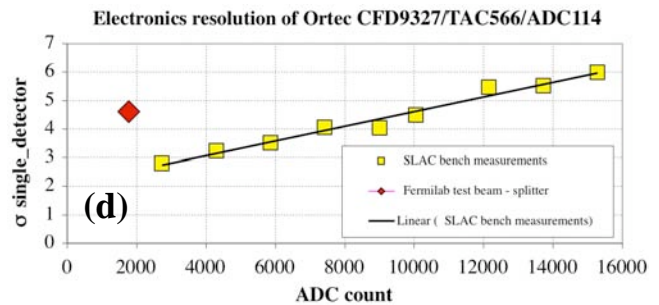
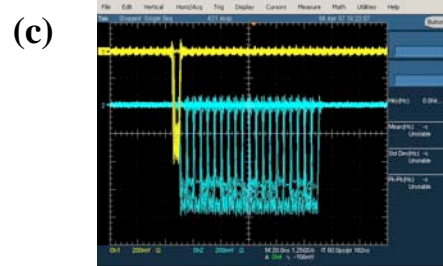
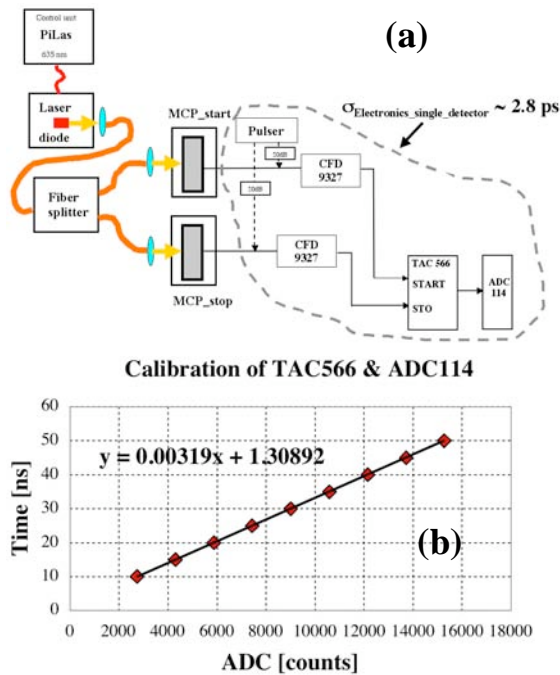


Fig. 3. (a) Lab setup to measure the time calibration and the electronics resolution (the MCP-PMTs were disconnected in this test). (b) Time calibration of the Ortec TAC/ADC system. (c) The output of the special calibration pulser. (d) The electronics resolution depends on where the peak is located in the ADC. In case of the lab test (squares), the setup was as in (a). In the Fermilab test (diamond), a high BW analog splitter was used to feed a TOF1 MCP-PMT output to both Start and Stop circuits.

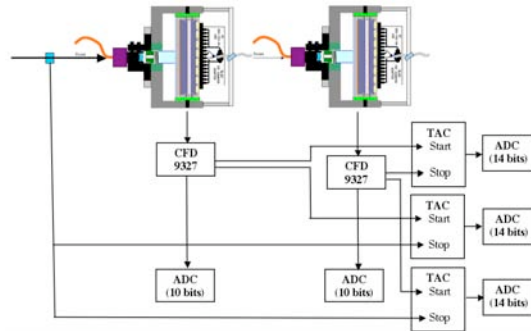


Fig. 4 Electronics setup used in the Fermilab test. It uses the same Ortec electronics, but in addition, we used LeCroy2249 ADCs to monitor the MCP pulse height.

⁸ We used the resistor chain values: 500k Ω :5MW:500k Ω .

⁹ The MCP-PMT voltages were 2.2 kV (TOF1) & 2.0 kV (TOF2) in the Fermilab test. In the SLAC test we tried several voltages close to these values.

3. Experimental results with a laser diode

Ref. 1 describes results using the laser diode in more detail. The tests used a laser diode¹⁰ with an 80:10:10 fiber splitter (Fig.3a). The single detector resolution is obtained by dividing the measured resolution by $\sqrt{2}$. The laser diode optics produced a 1 mm spot on the MCP face. The laser tests at low gain simulated the detector running conditions as used in the test beam: Fig.5a shows the measured resolution as a function of the number of photoelectrons¹¹ (Npe) at low gain for the CFD arming thresholds of -10 mV, the CFD walk (zero-crossing) threshold of $+5$ mV and MCP-PMT voltages of 2.28 & 2.0 kV respectively, and compares it with a prediction.¹² The prediction agrees well with the data if we assume that the transit time spread (the resolution for a single photoelectron) is σ_{TTS} (extrapolated to $N_{pe} = 1$) ~ 120 ps; such a large value of σ_{TTS} is consistent with our choice of low gain operation in order to be linear for signals of up to $N_{pe} \sim 30-50$, where we measure $\sigma_{\text{Single_detector}} \sim 20$ ps, see Fig.5a. Fig.5b shows an extrapolation to $N_{pe} = 1$ in a log-log representation.

Figures 5a-e show the resolution as a function of gain. One can see that the $1/\sqrt{N_{pe}}$ dependence is only approximate as the amplifier saturates at large gain and N_{pe} values, and we use it for eye guidance only. The resolution generally improves as one increases the gain. Fig. 5e shows the results at highest gain of $\sim 10^6$ with a full single photoelectron sensitivity. As one increases N_{pe} , the resolution is initially worse for $N_{pe} \sim 2-15$, then it improves for $N_{pe} > 30$; at that point the amplifier is fully saturated. An attempt to set the gain to one by placing a 20 dB attenuator in front of the 9327 CFD did not improve the resolution for large N_{pe} . It therefore appears that the best one can do is $\sigma_{\text{Single_detector}} \sim 12$ ps for $N_{pe} \sim 30-50$. This type of tuning is clearly dependent on the choice of electronics and the detector.

The limiting resolution at very large $N_{pe} \sim 250$ in Fig. 5a is found to be $\sigma_{\text{Single_detector}} \sim 5.0$ ps. We estimate that the MCP-PMT contribution to this

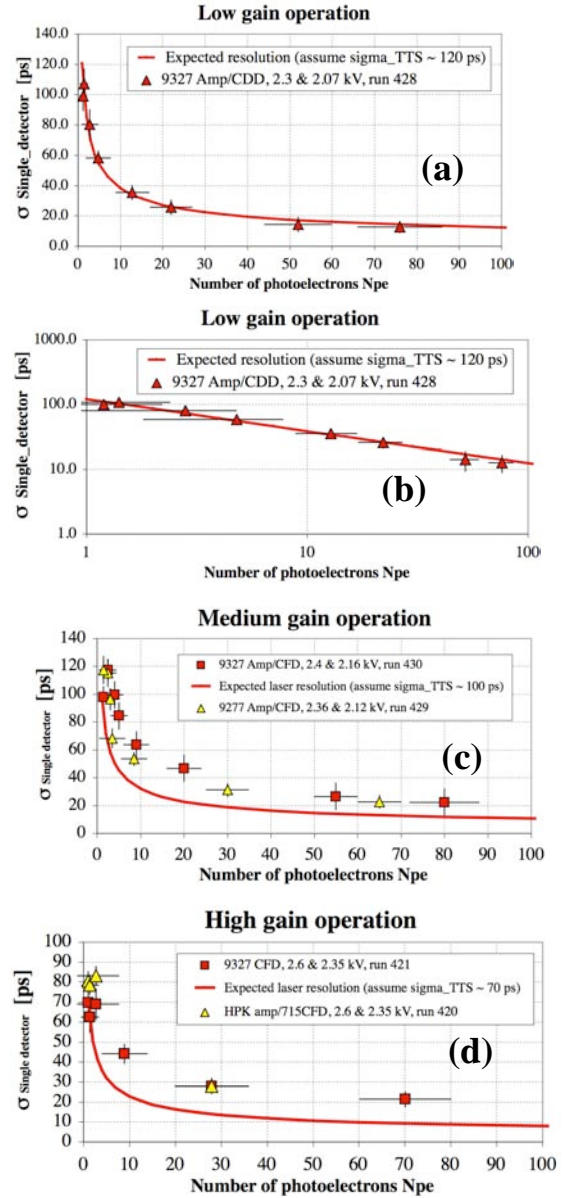
¹⁰ PiLas laser diode, 635 nm, $\text{FWHM}_{\text{Laser_diode}} \sim 32$ ps at 1 kHz.

¹¹ Laser diode light was attenuated by Mylar attenuators and N_{pe} was determined by several methods: (a) scope, (b) ADC measurement, and (c) statistical arguments.

¹² **Laser tests only:** $\sigma \sim \sqrt{[\sigma_{\text{MCP-PMT}}^2 + \sigma_{\text{Laser}}^2 + \sigma_{\text{Electronics}}^2]} \sim \sqrt{[\sigma_{TTS}/\sqrt{N_{pe}}]^2 + ((\text{FWHM}_{\text{Laser_diode}}/2.35)/\sqrt{N_{pe}})^2 + (\sigma_{\text{Electronics}})^2}$.

result is $\sigma_{\text{MCP-PMT}} < 4.5$ ps.¹³

Fig.5f shows the calibration of N_{pe} as a function of number of attenuators, which are used to adjust the light intensity. Fig.5g shows the gain dependence on voltage for both detectors.



¹³ MCP-PMT contribution to resolution: $\sigma_{\text{MCP-PMT}} < \sqrt{1/2 \{ \sigma_{\text{Electronics}}^2 - \sigma_{\text{Pulsar}}^2 \}} < 4.5$ ps, where $\sigma \sim 7.0$ ps, $\sigma_{\text{Pulsar}} \sim 2$ ps, and $\sigma_{\text{Electronics}} = 3.42$ ps, $\sigma_{\text{Single_detector}} = 7.0 \text{ ps}/\sqrt{2} = 5.0$ ps.

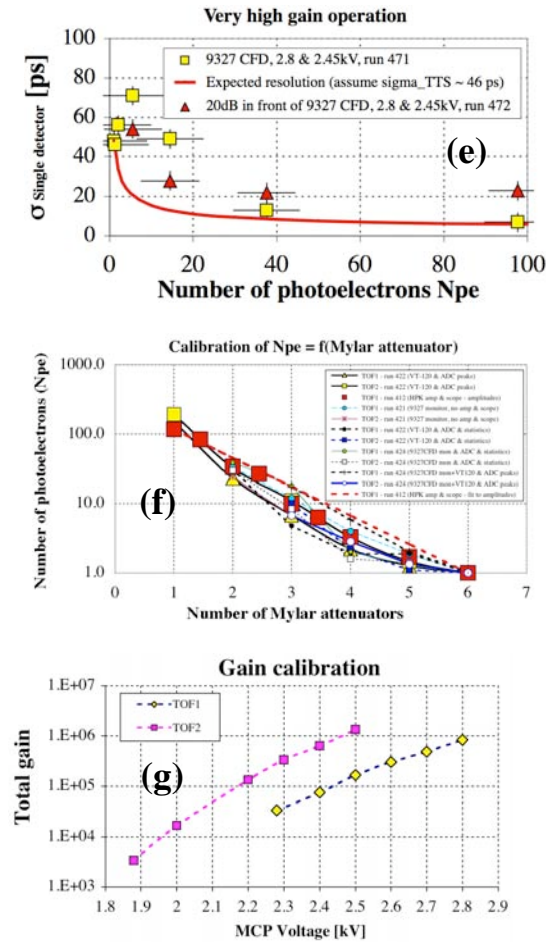


Fig. 5 (a) Measured laser diode timing resolution as a function of number of photoelectrons (N_{pe}) and gain. Solid curves show the calculation assuming $\sigma_{\text{TTS}} \sim 120$. (b) the same as (a) but in log-log representation. (c)-(e) The same as (a), but vary gain and assume different σ_{TTS} . (f) Calibration of N_{pe} as a function of the number of attenuators in the laser diode light using different methods: (i) oscilloscope, (ii) ADC, (iii) statistical argument. (g) Gain curves for the two detectors used in all tests described in this paper. Both detectors had MCP holes of $10 \mu\text{m}$ dia.

One should point out that the PiLas laser is not a limiting factor in our laser resolution measurements. PiLas company streak camera measurement for this particular laser diode indicates FWHM ~ 32 ps for 1 kHz frequency and the same tune choice (generally the laser diode timing resolution and its tail depend on the laser diode frequency, power, and a type of

diode). This means that the laser diode contributes $\sigma_{\text{Laser_diode}} \sim 13.6$ ps to the TTS measurement in our case, which gets divided by $\sqrt{N_{pe}}$ for larger number of photoelectrons. This means that we can measure σ_{TTS} of our MCP-PMTs. Fig.6 shows our best result of the σ_{TTS} measurement for the TOF1 detector at very high gain (2.8 kV) [2]. The tail of the distribution is composed of both (a) laser diode contribution and (b) photoelectron recoils from top MCP surface. If we subtract a contribution from the laser diode $\sigma_{\text{Laser_diode}}$ and the TDC resolution (25 ps/count), we get $\sigma_{\text{TTS}} \sim 28$ ps for the TOF1 MCP-PMT detector. Therefore both TOF detectors used in this paper can reach a very good TTS performance at very high gain. However, as pointed out earlier, we have chosen to operate the detectors at very low gain.

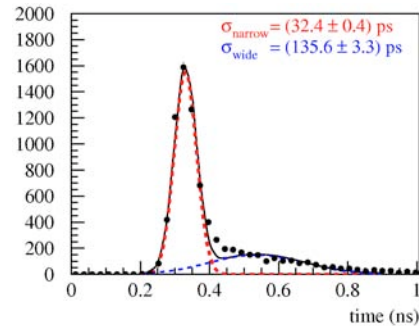


Fig. 6 Single photoelectron timing resolution of TOF1 counter with the laser diode used in this paper. The data obtained at very high gain of $\sim 10^6$ at 2.8 kV, HPK C5594-44 amplifier with a gain of 63x, Phillips 715 CFD and LeCroy TDC2248, and for single pad connected, while the rest of them grounded.

4. Experimental results with the test beam

The first beam test was done in a 10 GeV/c electron beam at SLAC. We found that the aluminum coating of the quartz radiator rods was not uniform, and therefore, we expected that the number of photoelectrons would be somewhat smaller, which explains the worse timing resolution of $\sigma_{\text{Single_detector}} = [10.73 \text{ counts} \times 3.19 \text{ ps/count}] / \sqrt{2} \sim 24$ ps, as shown in Fig.7a. This plot contains all events, i.e., no cuts on the MCP pulse heights, nor the ADC correction to the CFD timing are involved. Fig.7b shows perfect timing stability during the run.

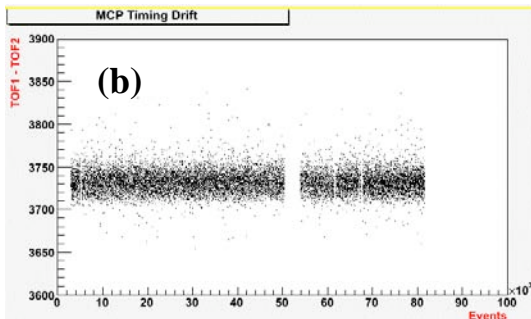
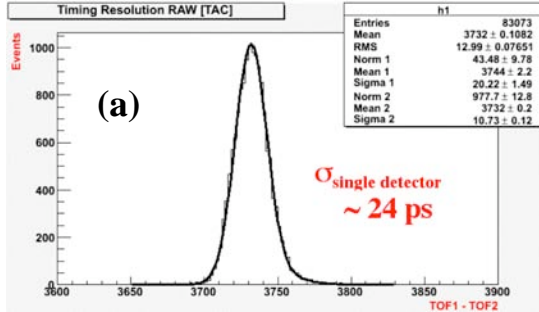


Fig. 7 (a) The single-detector resolution obtained in a 10 GeV electron beam at SLAC with the Photonis MCP-PMT setup shown on Fig. 1. Both detectors had MCP holes of $10 \mu\text{m}$ dia. No off-line ADC-based correction was applied, i.e., we accepted all events. (b) Timing stability during the SLAC beam run was excellent.

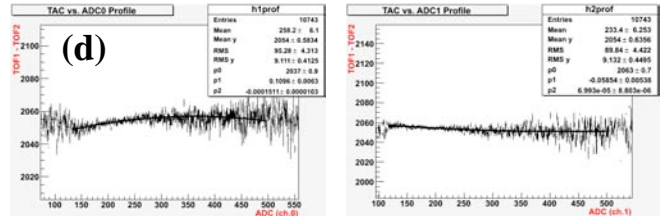
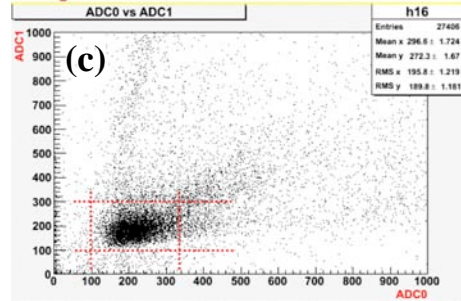
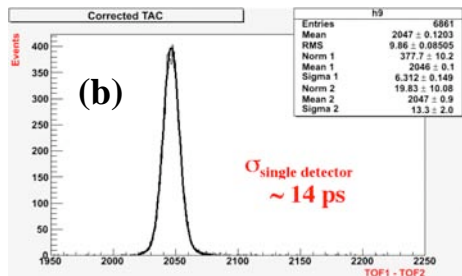
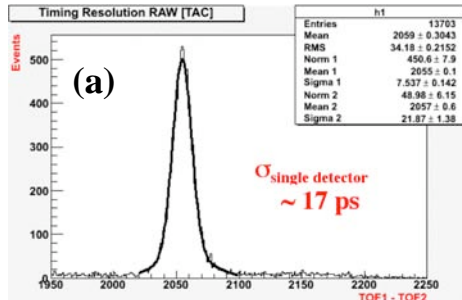


Fig. 8 (a) The single-detector resolution obtained in a 120 GeV proton beam at Fermilab with the Photonis MCP-PMT. Both detectors had MCP holes of $10 \mu\text{m}$ dia. No off-line correction to the CFD timing, and accepting all events. (b) The same result, but applying time-to-ADC correction to the CFD timing, and applying tight ADC cuts, as shown in (c) and (d).

The second beam test was done in a 120 GeV/c proton beam at Fermilab. This time the detectors had improved radiator coating.¹⁴ In addition, as we described in Fig.4, this test implemented the ADC off-line corrections. Fig.8a shows the results for all events without any ADC cut or CFD time-walk correction. This result is to be compared to Fig.7a. Fig.8b shows the final resolution of $\sigma_{\text{single_detector}} = [6.312 \text{ counts} \times 3.19 \text{ ps/count}] / \sqrt{2} \sim 14 \text{ ps}$, corresponding to tight cuts on the MCP-PMT pulse heights, shown in Fig.8c, and the time-walk correction to the CFD timing, shown on Fig.8d. The results clearly indicate that one has to be careful losing photoelectrons, and that the CFD needs to be corrected for the time-walk, to achieve the ultimate resolution.

Taking advantage of the pulse height measurement used in the Fermilab test, one can estimate the number of photoelectrons. Fig.9 shows the ADC spectra and resulting expected Npe statistics

¹⁴ Aluminum coating of the sides was made by the Photonis Co

from both MCP-PMT detectors. It indicates that a number of N_{pe} is about 23-25 on average. As was mentioned earlier, a calculation gives an estimate of $\sim 35 \pm 5$ photoelectrons for the average of the two detectors, taking into account all known efficiencies and degradation factors shown in Fig.2.¹⁵

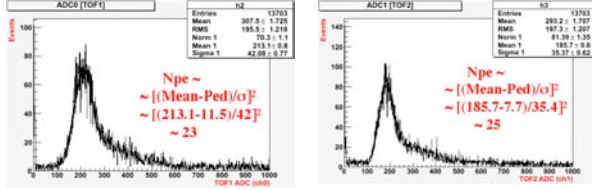


Fig. 9 Pulse height spectra from each TOF detector during the Fermilab beam test, corresponding to Fig.8. It shows the number of expected photoelectrons determined from the statistics of the pulse height spectra during the beam test.

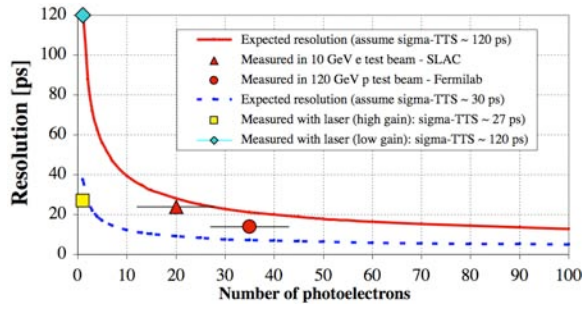


Fig. 10 Comparison of the SLAC & Fermilab test beam data and the simple model, assuming the “extrapolated” σ_{TTS} of 120 ps for low gain operation (diamonds) – see Fig.5a. The graph also shows the simple model assuming σ_{TTS} measurement with a laser diode at very high gain (square) [2].

Fig.10 compares the data in both beam tests with a simple model¹⁶ parameterized as a function of the calculated number of photoelectrons (N_{pe}). We quote the calculated N_{pe} to be 35 ± 5 for the Fermilab beam test. The predicted curve assumes a value of σ_{TTS} (extrapolated to N_{pe} = 1) ~ 120 ps, which is consistent with a low gain measurement shown on

¹⁵ The oscilloscope-based measurement would indicate a higher value of N_{pe} = 45 ± 10 ; this discrepancy could be related to several less known corrections in the oscilloscope test.

¹⁶ **Beam test:** $\sigma \sim \sqrt{[\sigma_{MCP-PMT}^2 + \sigma_{Radiator}^2 + \sigma_{Pad}^2 + \sigma_{Electronics}^2]} \sim \sqrt{[(\sigma_{TTS}/\sqrt{N_{pe}})^2 + ((L/\cos\Theta_C)/(300\text{mm/ps})/n_{group})/\sqrt{(12N_{pe})^2 + ((L_{pad}/300\text{mm/ps})/\sqrt{(12N_{pe})^2 + \sigma_{Electronics}^2})}]}$, where L is a radiator length, L_{pad} is a pixel size, N_{pe} is a number of photoelectrons, and n_{group} is a group refraction index.

Fig.5a. Fig.10 also shows the measured σ_{TTS} of ~ 28 ps [2], obtained at very high gain operation, and a corresponding model’s prediction. If this is the case, one could achieve, in principle, a timing resolution of ~ 10 ps for N_{pe} ~ 15 , and therefore one could use a thinner radiator. This limit was not reached with this particular detector/electronics setup in our laboratory tests. There is a hint, however, from Fig.5d that one should set the amplifier gain to unity if one wants to use the 9327 CFD.

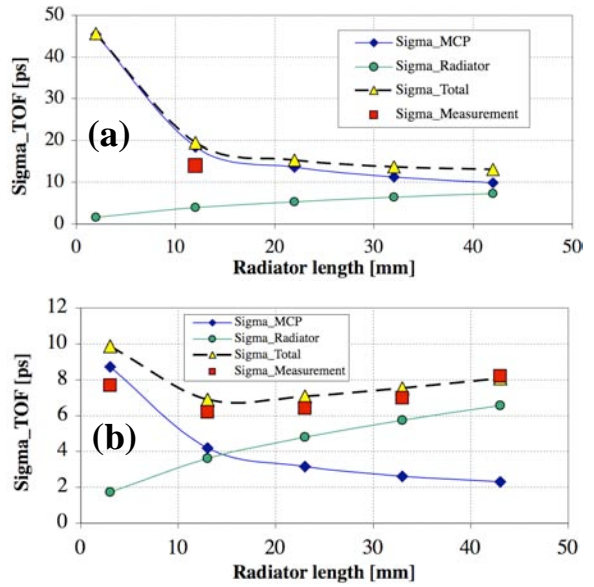


Fig. 11 (a) A comparison of the Fermilab test beam result and a prediction of the resolution as a function of the radiator length, assuming the “extrapolated” measurement of $\sigma_{TTS} \sim 120$ ps and 35 pe/10mm radiator length. (b) The same for the Nagoya test, assuming $\sigma_{TTS} \sim 32$ ps and 45 pe/10mm radiator length [9].

It is interesting to ask how the resolution depends on the radiator length. We use a simple model,¹⁷

¹⁷

Fermilab beam test - σ_{TTS} (extrapolate to N_{pe} = 1) = 120 ps:
 $\sigma_{TOF} \sim \sqrt{[\sigma_{MCP-PMT}^2 + \sigma_{Radiator}^2 + \sigma_{Pad\ broadening}^2 + \sigma_{Electronics}^2]} = \sqrt{[(\sigma_{TTS}/\sqrt{N_{pe}})^2 + ((L*1000\mu\text{m}/\cos\Theta_C)/(300\mu\text{m/ps})/n_{group})/\sqrt{(12N_{pe})^2 + ((2*1000\mu\text{m}/300\mu\text{m/ps})/\sqrt{(12N_{pe})^2 + (4.6\text{ ps})^2})}]}$
 For L = 12 mm: $\sigma_{TOF} \sim \sqrt{[18.5^2 + 3.9^2 + 0.3^2 + 4.6^2]} \sim 19.5$ ps
Nagoya beam test [9] - σ_{TTS} (N_{pe} = 1) = 32 ps (high gain):
 $\sigma_{TOF} \sim \sqrt{[\sigma_{MCP-PMT}^2 + \sigma_{Radiator}^2 + \sigma_{Pad\ broadening}^2 + \sigma_{Electronics}^2]} = \sqrt{[(\sigma_{TTS}/\sqrt{N_{pe}})^2 + ((L*1000\mu\text{m}/\cos\Theta_C)/(300\mu\text{m/ps})/n_{group})/\sqrt{(12N_{pe})^2 + ((5*1000\mu\text{m}/300\mu\text{m/ps})/\sqrt{(12N_{pe})^2 + (4.1\text{ ps})^2})}]}$
 For L = 13 mm: $\sigma_{TOF} \sim \sqrt{[4.18^2 + 3.6^2 + 0.63^2 + 4.1^2]} \sim 6.9$ ps

which assumes a $1/\sqrt{N_{pe}}$ dependence, for both tests, i.e. our Fermilab test and compare it to the Nagoya test [9]. This model neglects the fact that the later arriving photoelectrons from a longer radiator may contribute smaller weight to the timing resolution, especially for a very high gain operation as in the case of Fig.11b [9]. For the low gain operation the $1/\sqrt{N_{pe}}$ dependence seems to work – see Fig.5a,b. One concludes that a 10 mm radiator length is a reasonable choice for the low gain operation; a high gain operation would allow shorter length.

Several other fast MCP-PMT detectors were tested in the test beam at the same time and gave similar excellent results [7, 8]. This will be described in a separate future publication.

To conclude, we have shown that it is possible to achieve a quite good TOF timing resolution with a low gain MCP-PMT operation. Such a detector would not see a single photoelectron background, it would be sensitive only to charged particles, and therefore it might have smaller aging problems. This is a departure from a previously chosen technique to run a TOF detector at a very high gain and with a single photoelectron sensitivity [9]. The aging tests at low gain are in progress.

Acknowledgments

We would like to thank M. McCulloch for help to prepare the detector setup. We thank H. Frisch, Paul Hink and Emile Schyns for useful advice and help.

References

- [1] J. Va'vra, C. Ertley, D.W.G.S. Leith, B. Ratcliff, and J. Schwiening, Nucl. Instr.&Meth., A595(2008)270-273.
- [2] J. Va'vra, J.F. Benitez, D.W.G.S. Leith, G. Mazaheri, B. Ratcliff and J. Schwiening, "A 30 ps timing resolution for single photons with multi-pixel Burle MCP-PMT," Nucl. Instr.&Meth., A572(2007)459-462.
- [3] Super-B CDR report, INFN/AE-07/2, SLAC—856, LAL07-15, March 2007.
- [4] A. Lehman et al., Nucl. Instr. & Meth., A595(2008)335.
- [5] J. Va'vra, J. Benitez, D.W.G.S. Leith, G. Mazaheri, B. Ratcliff, J. Schwiening, and K. Suzuki, "The Focusing DIRC – the first RICH detector to correct the chromatic error by timing, and the development of a new TOF detector concept", SLAC-PUB-12803, March, 2006.
- [6] J. Benitez, I. Bedajenek, D.W.G.S. Leith, G. Mazaheri, B.N. Ratcliff, K. Suzuki, J. Schwiening, J. Uher, and J. Va'vra, "Development of a Focusing DIRC," IEEE Nucl. Sci., Vol. 3, pp. 1550-1556, Conference Record, October 2006, and SLAC-PUB-12236.
- [7] E. Ramberg, "An in-depth look at the latest PSec test beam results," All experimenters seminar, Fermilab, August 25, 2008.
- [8] K. Byrum "Psec Level Time-of-Flight Measurements at Argonne's Laser Lab and Fermilab's Test Beam", Picosecond timing workshop, Lyon, France, October 2008
- [9] K. Inami, H. Kishimoto, Y. Enari, M. Nagamine, and T. Ohshima, "A 5 ps TOF-counter with MCP-PMT", Nucl. Instr. & Meth., A560(2006)303-308, and A564(2006)204.